European Journal of Medicinal Chemistry 108 (2016) 28–38

Contents lists available at ScienceDirect

European Journal of Medicinal Chemistry

journal homepage: http://www.elsevier.com/locate/ejmech

Research paper

Synthesis and evaluation of gallocyanine dyes as potential agents for the treatment of Alzheimer's disease and related neurodegenerative tauopathies

Spyros Mpousis [a, 1], Savvas Thysiadis [a, 1], Nicolaos Avramidis [b, 1], Sotirios Katsamakas [c], Spiros Efthimiopoulos [b, **], Vasiliki Sarli [a, *]

[a] Department of Chemistry, Aristotle University of Thessaloniki, University Campus, 54124, Thessaloniki, Greece
[b] Division of Animal and Human Physiology, Department of Biology, National & Kapodistrian University of Athens, Panepistimiopolis, Ilisia, Greece
[c] Department of Pharmaceutical Chemistry, School of Pharmacy, Aristotle University of Thessaloniki, University Campus, 54124, Thessaloniki, Greece

ARTICLE INFO

Article history:
Received 16 June 2015
Received in revised form
27 October 2015
Accepted 17 November 2015
Available online 22 November 2015

Keywords:
Gallocyanine
Phenoxazine
DKK1 inhibitors
DKK1/LRP6 interaction inhibitors
Tau phosphorylation inhibition
Alzheimer's disease
Tauopathies

ABSTRACT

In search of safe and effective anti-Alzheimer disease agents a series of gallocyanine dyes have been synthesized and evaluated for their ability to inhibit LRPs/DKK1 interactions. Modulation of the interactions between LRP_S and DKK1, regulate Wnt signaling pathway and affect Tau phosphorylation. The current efforts resulted in the identification of potent DKK1 inhibitors which are able to inhibit prostaglandin J2-induced tau phosphorylation at serine 396.

1. Introduction

Alzheimer's disease (AD) is the most common neurodegenerative disease characterized by excessive accumulation of senile plaques and neurofibrillary tangles (NFT) [1]. Senile plaques are composed mainly of beta-amyloid peptide (Aβ) and neurofibrillary tangles of hyperphosphorylated microtubule-associated Tau protein [2]. Recent findings have established that deregulation of Wnt signaling contributes to the pathophysiology of AD, while activation of the pathway is neuroprotective [3]. According to Hanger and Noble the kinase activity of GSK3β is inhibited following activation of Wnt signaling, implicating this pathway in the hyperphosphorylation of Tau and the formation of NFTs [4].

Wnt signaling is initiated when Wnt proteins simultaneously interact with their receptor and co-receptor, Frizzled (FRZ) and LRP5/6. Through several cytoplasmic components, the signal is transduced to GSK3β with a subsequent stabilization of beta-catenin, which in turn enters the nucleus and forms a complex with TCF/LEFs to activate transcription of target genes [5a]. In the absence of Wnt, phosphorylation of beta-catenin by GSK3β leads to ubiquitination and subsequent proteasomal degradation, resulting in low levels of cytoplasmic beta-catenin [5b]. The canonical Wnt pathway is also negatively modulated by the extracellular protein Dickkopf-1 (DKK1), which binds to LRPs preventing their interaction with Wnts and Frizzled membrane receptor [6]. The Dickkopf family encodes secreted proteins of 255–350 aminoacids and

Abbreviations: AD, Alzheimer's disease; NFT, neurofibrillary tangles; Aβ, beta-amyloid peptide; FRZ, frizzled; DKK1, Dickkopf-1; GSK3β, glycogen synthase kinase-3 beta; TCF, T-cell factor; LEF, lymphoid enhancer factor; BBB, blood–brain barrier; PGJ2, prostaglandin J2; LRP6, low-density lipoprotein receptor-related protein 6; Wnt, wingless; CNS, central nervous system; p53, tumor protein p53; IL-1β, interleukin-1 beta; NCI, National Cancer Institute; HB, hydrogen bond; HBD, hydrogen bond donor; HBA, hydrogen bond acceptor; DMSO, dimethyl sulfoxide; MTT, 3-(4,5-dimethylthiazol-2-yl)-2,5-diphenyltetrazolium bromide; PK, pharmacokinetic.

* Corresponding author.
** Corresponding author.
E-mail addresses: efthis@biol.uoa.gr (S. Efthimiopoulos), sarli@chem.auth.gr (V. Sarli).

[1] These authors contributed equally.

http://dx.doi.org/10.1016/j.ejmech.2015.11.024
0223-5234/

consists of four main members (DKK-1 to -4) in mammals [7]. Sokol and coworkers have reported that the DKK C-terminal domain mainly interacts with the third and fourth propellers of LRP5/6 and these interactions are necessary and sufficient for Wnt inhibition [8].

The expression of DKK1 is increased in brains of AD patients and in AD transgenic mouse models and this induction is dependent on p53 and associated with neurodegeneration [9,10]. In cultured neurons, DKK1 is able to elicit cell death associated with loss of BCL-2 expression, induction of BAX, and Tau hyperphosphorylation [11]. Along these lines, a recent study demonstrated that DKK1-neutralizing antibodies suppress Aβ-induced synapse loss in mice [12]. Thus, modulation of the interactions between LRPs and DKK1, could regulate Wnt-beta-catenin signaling offering an attractive therapeutic approach for treating AD. In fact the LRP5-DKK1 interaction has been recently targeted with monoclonal anti-DKK1 antibodies [13]. However, the lack of blood brain penetration of the antibodies limits their application for the treatment of CNS diseases.

In this study, a small molecule approach for regulating Wnt signaling has been developed. Based on NCI8642, a recently discovered compound which blocks DKK1 inhibitory activity by disrupting DKK1/LRP6 interactions, a series of NCI8642 derivatives have been synthesized and evaluated. Importantly, this study shows that NCI8642 and related analogues induce inhibition of tau phosphorylation *in vivo*. Since tau hyperphosphorylation is a hallmark of Alzheimer's disease these results may find application in the treatment of AD and other tauopathies.

NCI8642 (**1a**, gallocyanine hydrochloride salt), a synthetic blue dyestuff synthesized by Otto in 1888 [14], is a phenoxazinone (see Scheme 1) independently discovered as an inhibitor of DKK1-LRP5/6 interactions by the groups of Remelli [15], Zheng and Wu [16]. Phenoxazines are privileged compounds, present in several bioactive molecules and natural products that display diverse biological activities. Well-known examples are the natural products actinomycins, which are polypeptide antibiotics produced by Streptomyces species that show chemotherapeutic activity in a number of neoplastic diseases [17]. The phenoxazine template is also present in the plectosphaeroic acids isolated from the fungus *Plectosphaerella cucumerina*, which are inhibitors of indoleamine 2,3-dioxygenase [18]. Simpler phenoxazines and benzophenoxazines have well documented anticancer [19–21], antiviral [22], antimicrobial [23] and antimalarial [24,25] properties. Importantly, phenothiazine compounds have also been reported to inhibit heparin-induced assembly of tau protein [26].

Among the known Wnt modulators, NCI8642 is the only DKK1 inhibitor described so far, but its use as a clinically suitable drug is limited, because its association with LRP6 is weak (IC50 of about 3 μM in the inhibition of DKK1 binding). Nevertheless, data show that NCI8642 is effective *in vivo* as it reduces basal blood-glucose concentrations and improves glucose tolerance in mice [16]. NCI8642 possess both acidic and basic groups and a mesomeric chromophoric system which is depicted in Scheme 2 [27].

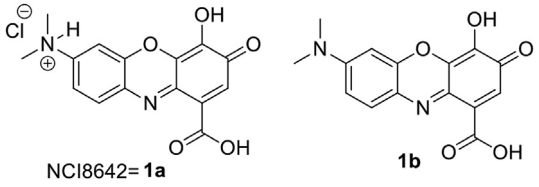

Scheme 1.

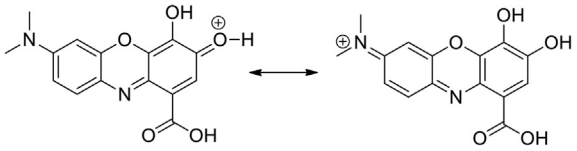

Scheme 2.

2. Results and discussion

2.1. Docking studies

In an attempt to gain insight into the structural basis of the observed activity, NCI8642 and related analogues were docked against LRP6. Previous publications have demonstrated that NCI8642 binds to LRP6 and inhibits DKK1-LRP6 binding by using biolayer interferometry and surface plasmon resonance technology (SPR) [15,16]. Accordingly, the heterotetramer structure 3S8V in the absence of DKK1c module (PDB code: 3S8V) was used in the present studies [28]. The docking results show top scoring poses in LRP6-E3E4/DKK1 interfaces consisting of the residues Ser851, Asp874 in interface A and Trp850, Asp874, Tyr875 in interface B. For the screened compounds a repeated motif for their calculated binding was witnessed. The phenoxazine was proved a privileged scaffold for LRP6, due to a versatile interaction either through the nitrogen or oxygen atom with Tyr875 of interface A, in a binding pocket which is mainly hydrophobic and occupied by Leu231 of the DKK1c module in the LRP6/DKK1 complex. In Fig. 1 three major binding modes of NCI8642 are illustrated: two poses with the dimethylamino group to extend towards Ser851 and one pose with the ammonium ion to display ionic interactions with Asp874.

In an effort to extract a qualitative probability profile for each solution, we decided to synthesize analogues that added hindering effects towards the hydrophobic region of the pocket (*e.g.* **7b**, **7e**, Scheme 3) or analogues that lacked characteristic groups (*e.g.* **4a**, **4j**, Scheme 3) which appeared to participate through HB forming interactions, while constantly maintaining the original scaffold. In addition, a series of ester derivatives were chosen to be tested in an effort to increase hydrophobicity and mimic Leu231 of DKK1. Besides the phenoxazine privileged scaffold, of almost equal significance to the binding orientation of the tested compounds appeared to be the presence of the ammonium salt. Notably, the tested structures displayed several HBs that are generally maintained in different poses, while the salts exhibited the usual HBs with an extra possible ion interaction with length bellow a 4 $Å^3$ threshold [30], between the positively charged nitrogen and the anionic region of the pocket formed by the two aspartic residues, Asp874A and Asp874B. These docking results have to be verified from real biological data.

2.2. Synthesis of gallocyanine dyes

The synthesis of gallocyanine derivatives was performed as depicted in Scheme 3. Initially, the preparation of **4a** took place from the decarboxylation of commercially available gallocyanine **1a** was achieved using CH_3COONa in water and heating according to Šimek and coworkers [27]. Next, *N,N*-dialkyl-4-nitrosoaniline hydrochloride salts **2** and **6** were allowed to react with commercially available phenols **3i**, **3j** or with gallate esters to give the corresponding phenoxazinones **4b**–**j**, **7b** and **7e**. It should be noted that, the nitroso compounds **2** and **6** were prepared following the method of G. M. Bennett and E. V. Bell [31]. Compounds **3b**–**f** were synthesized according to known procedures [32–35] whereas the synthesis of **3g** and **3h** is described in the Supporting Information

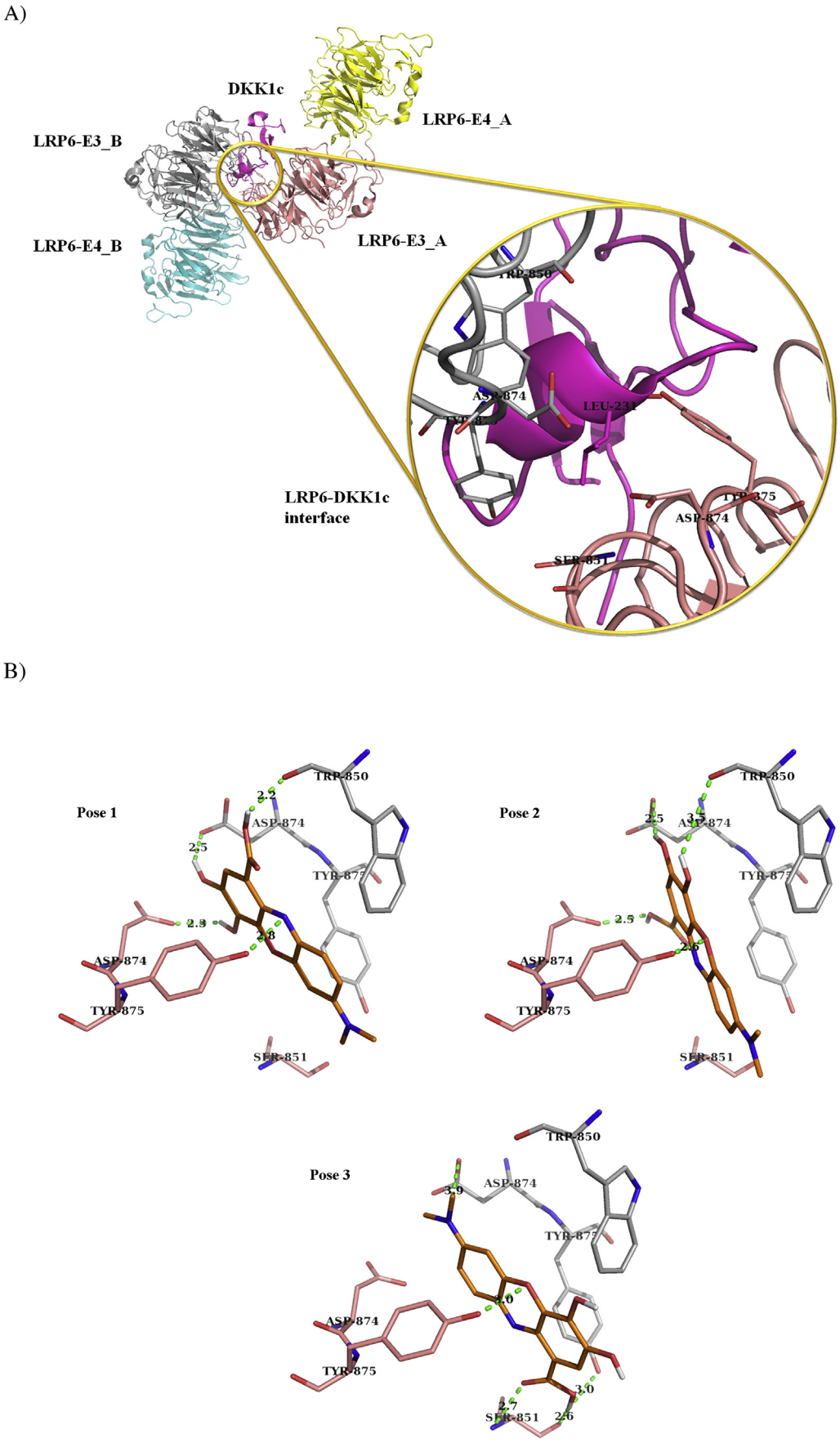

Fig. 1. (A) Crystal structure of LRP6-E3E4/DKK1 (PDB: 3S8V). The docking studies were performed in the highlighted LRP6-E3E4/DKK1 interfaces. (B) *In silico* docking results. Three highest rank poses of NCI8642 (gold sticks) docked into LRP6 (pink-interface A, grey-interface B). Critical hydrogen bonding residues are labeled. The figures were obtained by PyMol version 1.4.1 [29].

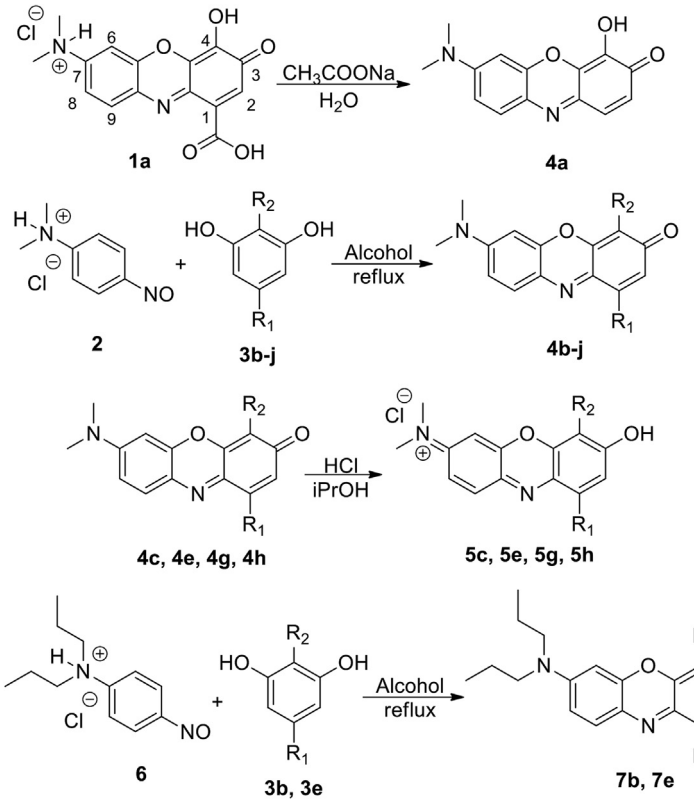

a) R_1=H, R_2=OH
b) R_1=CO_2Me, R_2=OH
c) R_1=CO_2Et, R_2=OH
d) R_1=CO_2*i*-Pr, R_2=OH
e) R_1=CO_2*n*-Bu, R_2=OH
f) R_1=CO_2Bn, R_2=OH
g) R_1=$CO_2(CH_2)_2OCH_3$, R_2=OH
h) R_1=CO_2*n*-hexyl, R_2=OH
i) R_1= CH_3, R_2=H
j) R_1=OH, R_2=H

Scheme 3. Synthesis of gallocyanine dyes.

section. Ammonium salts **5c**, **5e**, **5g** and **5h** were synthesized from the corresponding amines after treatment with HCl in iPrOH.

3. Biological evaluation

3.1. The effect of NCI8642 and related derivatives on the binding of DKK1 to the surface of HEK-293 cells overexpressing LRP6

In order to examine the effect of NCI8642 and related derivatives on the binding of DKK1 on the surface of HEK-293 cells overexpressing LRP6 (HEK-293LRP6), sub-confluent cultures were incubated with DKK1 conditioned medium (DKK1-CM) plus DMSO, 100 μM NCI8642 or 100 μM NCI8642 derivatives for 2 h at 4 °C [15]. Cell surface binding of DKK1 was visualized by immunocytochemistry using a primary anti-DKK1 antibody and fluorescent secondary antibody. Fluorescence images were analyzed using Zen software and quantified results are shown in Fig. 2. The results derive from three independent experiments performed in duplicates. The average values represent measures of 750 cells for each case.

As it can been seen in Fig. 2 the compounds tested had the ability to inhibit DKK1-LRP6 interactions and most of them were equipotent or more potent than NCI8642. The presence of the hydrochloride salt was critical for inhibition as it was indicated in the increased activity of the free amino derivative **1b**. Compound **4a** lacking the carboxyl group on the phenoxazine template was found slightly more potent than **1a**. Next, the effects of ester compounds

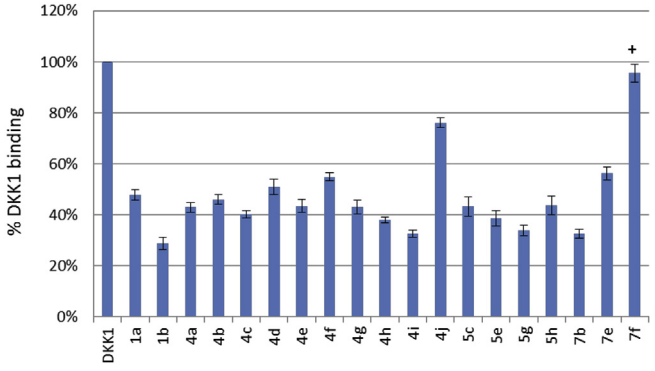

Fig. 2. The effect of NCI8642 and related derivatives on the binding of DKK1 to the surface of HEK-293 cells overexpressing LRP6 (HEK-293LRP6). HEK-293LRP6 cells were incubated with DKK1 conditioned medium (DKK1-CM) plus DMSO, NCI8642 or NCI8642 derivatives at a concentration of 100 μM for 2 h at 4 °C. Immunofluorescence images were used to quantify DKK1 binding at the cell surface using Zen software. The results are expressed as percentage of DKK1 binding. The experiment was repeated three times in duplicates and 750 cells were analyzed in each case. The differences are statistically significant (p value <0.01). If not, they are indicated as (+). **7f** = ethyl gallate.

which include various lengths of alkyl side chains on the inhibition of DKK1-LRP6 interactions were examined. The data show that the inhibitory activity was dependent on the length of the alkyl chain and minor increases in potency were observed with higher alkyl

homologues such as the hexyl derivative **4h**. The methoxyethyl ester **4g** was equally potent inhibitor with the butyl analogue **4e**, while transformation of the carboxylate moiety to a benzyl ester provided a poor DKK1 inhibitor. In addition, compound **4j** lacking the carboxyl group and having a hydroxyl group at position 1 of phenoxazine template was less potent than **1a**, while compound **4i** lacking the hydroxyl group and carrying methyl group in the place of carboxyl group was an active compound.

To clarify the structure–activity relationships and improve the water solubility of the key analogues a series of simple ammonium salts were tested. Only, the hydrochloride salt **5g** afforded a significant improvement in inhibition over **4g**. The other salts tested **5c**, **5e** and **5h** were equally or less active than the corresponding free amines **4c**, **4e** and **4h**. Replacement of the dimethylamino by the dipropylamino group resulted in increased activity when the phenoxazine was carrying a methyl ester (**7b**) and in decreased activity in the case of the *n*-butyl derivative (**7e**). It should be noted that the ethyl gallate **7f** was also tested in this assay and was found completely inactive.

3.2. Cytotoxicity of the new compounds

The synthesized compounds were screened for their cytotoxic effects using the colorimetric MTT assay in order to determine the percentage of viable cells remaining following compound incubation at two different concentrations (10 and 100 μM) [36] After 24 h of cell culture, neuronal cells were not affected by the gallocyanine dyes since their viability was almost 100% (See Supporting Information Figure S1).

3.3. Prostaglandin J2 (PGJ2) induces tau phosphorylation at serine 396

In order to set up an assay of induced tau phosphorylation, we examined the effect of various immune factors IL-1β, lipopolysaccharide and PGJ2 on tau phosphorylation in mouse cortex primary neurons. IL-1β, and lipopolysaccharide did not induce tau phosphorylation at several sites that were examined. However, as indicated in Fig. 3, treatment of primary neurons with 10 or 20 μM PGJ2 resulted in a significant increase in tau phosphorylation at serine 396. Treatment with PGJ2 resulted also in tau hyperphosphorylation at other residues including serine 404, serine 199 and threonine 205 (data not shown).

The effect of selected NCI8642 derivatives on PGJ2-induced tau phosphorylation at serine 396 was subsequently examined. Primary cortical neurons were incubated with 20 μM PGJ2 plus DMSO, NCI8642 (10 μM) or NCI8642 derivatives (10 μM) for 1 h at 37 °C. Phosphorylation of tau was assayed by western blot using a pSer396 antibody. Quantification of the results normalized for actin is shown in Fig. 4. Importantly, the experiment shows that NCI8642

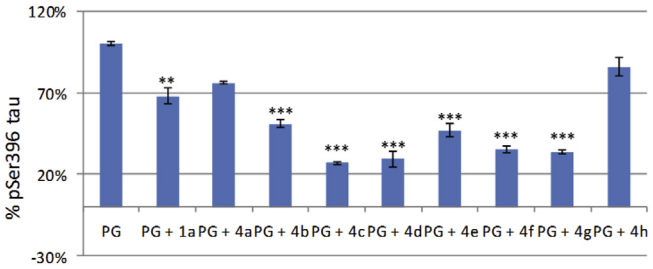

Fig. 4. Primary mouse cortex neurons were treated with 20 μM PGJ2 plus DMSO, 10 μM NCI8642 or 10 μM NCI8642 derivatives for 1 h at 37 °C. Cell lysates were analysed by western blot using antibodies against tau phosphorylated at serine 396 or actin. The density of the bands was measured using ImageJ software and the levels of tau phosphorylation at serine 396 were normalized to the levels of actin. The levels of phosphorylation upon combined treatment with PGJ2 plus the various NCI8642 derivatives are depicted as percent of tau phosphorylation upon treatment only with PGJ2. The experiments were repeated at least three times. The differences are statistically significant (***p value < 0.01, **p value < 0.025).

(**1a**) is able to reduce PGJ2-induced tau phosphorylation at serine 396. Ester derivatives **4b**–**h** were effective inhibitors of tau phosphorylation, with most potent the ethyl derivative **4c** which is 2.5 times as potent as NCI8642. The decarboxylated derivative **4a** and the hexyl ester **4h** were found less active than **1a**. Evidently, there is no good correlation between the effect of NCI derivatives on DKK1 binding and tau phosphorylation. This outcome may possibly be related to the fact that the tested NCI8642 derivatives may display diverse binding modes as was also initially observed from the docking studies. Some derivatives may bind to the DKK1 binding site and prevent DKK1 from binding. Some others may bind to the DKK1 binding site and act as an agonist of DKK1 while at the same time prevent binding of DKK1. The different potencies can also be associated to a non-selective activity of the tested compounds.

In an effort to evaluate the drug like profile of the synthesized compounds several PK properties were calculated as depicted in Table S1 (See Supporting Information). Generally, the phenoxazine scaffold poses a volume of 166 $Å^3$, and its substitution pattern is the key for a better DKK1 inhibition. The overall drug like profile shows a good partitioning and distribution coefficients, except from some violations of the lipophilicity mainly regarding to the ammonium salt derivatives. The polar surface area varied from approximately 60-100, HBD from 0 to 3, HBA from 4 to 8 and they appeared flat with Fsp^3 values between 0.13 and 0.43. This flexibility is mostly attributed to the presence of the long aliphatic substituents.

4. Conclusion

A series of novel gallocyanine dyes have been synthesized and evaluated for their ability to inhibit LRP/DKK1 interactions. Several

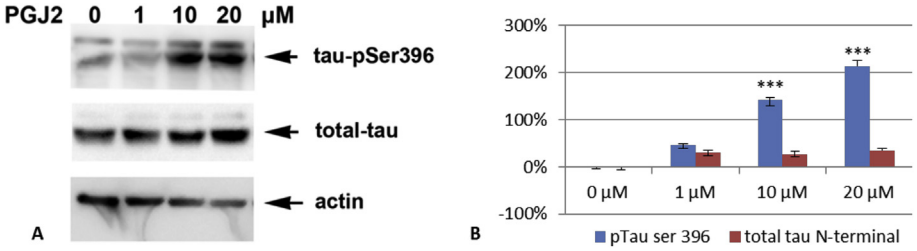

Fig. 3. A. Primary mouse cortex neurons were treated with 0, 1, 10 or 20 μM of PGJ2 for 1 h at 37 °C. Cell lysates were analysed by western blot using antibodies against tau phosphorylated at serine 396, N-terminus of tau (total tau) or actin. B. The density of the bands was measured using ImageJ software and the levels of tau phosphorylation at serine 396 were normalized to the levels of actin. The increase in the phosphorylation upon treatment with various concentrations of PGJ2 is expressed as percent of the levels of tau phosphorylation in untreated samples (0 μM PGJ2). The differences are statistically significant (***p value < 0.01).

compounds have been identified as more potent inhibitors than NCI8642 and important features for activity have been recognized. The present study further showed that NCI8642 and derivatives are able to inhibit prostaglandin J2-induced tau phosphorylation at serine 396. This finding is of particular importance and provides evidence that DKK1 may be a potential therapeutic target for treating AD and other tauopathies. Since, an x-ray structure of the NCI8642 with LRP6 is currently not available, a more detailed description of the relation between the chemical structures and the observed biological activities based only on docking simulations are not provided here. A binding mode validation of the inhibitors on LRP6 by X-ray structure determination and a larger number of inhibitors accompanied by their biological data are required for a detailed and valid SAR analysis. This project is on progress and will be reported in due course.

5. Experimental section

5.1. General experimental details

All reactions were carried out under an atmosphere of Ar unless otherwise specified. Commercial reagents of high purity were purchased and used without further purification, unless otherwise noted. Reactions were monitored by TLC and using UV light as a visualizing agent and aqueous ceric sulfate/phosphomolybdic acid, ethanolic p-anisaldehyde solution, potassium permanganate solution, and heat as developing agents. The ^{1}H and ^{13}C NMR spectra were recorded at 500 and 125 MHz, and tetramethylsilane was used as an internal standard. Chemical shifts are indicated in δ values (ppm) from internal reference peaks (TMS ^{1}H 0.00; $CDCl_3$ ^{1}H 7.26, ^{13}C 77.00; DMSO-*d6* ^{1}H 2.50, ^{13}C 39.51, pyridine-*d5* ^{1}H 8.74, 7.58, 7.22; ^{13}C 150.35, 135.91, 123.87). Melting points (mp) are uncorrected. High-resolution mass spectra (HRMS) were recorded by direct injection of a 2 μM (2 μl) solution of the compounds in water–acetonitrile (1/1; v/v) and 0.1% formic acid on a mass spectrometer (hybrid ion trap-orbitrap mass spectrometer) equipped with an electrospray ion source in positive mode (source voltage 3.5 kV, sheath gas flow 10, capillary temperature 275 °C) with resolution R = 60.000 at m/z = 400 (mass range = 150–2000) and dioctylphthalate (m/z = 391.28428) as the "lock mass".

The polyclonal/monoclonal Rabbit Anti-Mouse antibody kindly provided from Dr. Luc Buee (Insern, Fac de Medicine, Univ. Lille 2, Lille France) directed against the N-terminus of tau and the polyclonal Rabbit Anti-Mouse antibody detecting tau phosphorylated at serine 396 were purchased from Acris Antibodies GmbH (Germany). Goat Anti-Rabbit IgG-HRP secondary antibody was purchased from Jackson ImmunoResearch (Baltimore Pike, USA). The monoclonal Mouse antibody used to detect actin by immunoblot was purchased from Merk Millipore (Darmstatd, Germany). Goat Anti-Mouse IgG-HRP secondary antibody was purchased from Santa Cruz Biotechnology (Dallas/Texas, USA). The polyclonal Rabbit Anti-Human antibody against DKK1 was obtained from Santa Cruz Biotechnology (Dallas/Texas, USA). Goat anti-Rabbit IgG (H + L) Alexa Fluor 488-conjugated and/or Goat anti-Rabbit IgG (H + L) Cy 3-conjugated secondary was purchased from Jackson ImmunoResearch (Baltimore Pike, USA). B27 and Neurobasal used to culture mouse primary neuronal culture were purchased from Life Technologies (Grand Island/NY, USA). Prostaglandin J2 was purchased from Santa Cruz Biotechnology (Dallas/Texas, USA). Common chemicals were from Sigma Aldrich (Athens, Greece).

5.2. 7-(Dimethylamino)-4-hydroxy-3H-phenoxazin-3-one, ***4a***

Gallocyanine hydrochloride (1 g, 2.97 mmol) and sodium acetate (1 g, 12.19 mmol) were heated under reflux in water (100 mL) for 5 h. The reaction mixture was allowed to cool at 0 °C. The unreacted gallocyanine was taken up in of sodium carbonate solution, while the decarboxylated gallocyanine is insoluble. The precipitate was collected by filtration. To increase the purity, the solid was refluxed in ethanol (9 mL) for 10 min and stored at 8 °C overnight. The product was then collected by filtration as a dark blue solid (640 mg, yield 84%) [17]. **4a:** ^{1}H NMR (500 MHz, pyridine-d5) δ 7.67 (d, J = 8.9 Hz, 1H), 7.42 (d, J = 9.6 Hz, 1H), 7.03 (d, J = 9.6 Hz, 1H), 6.62 (d, J = 9.0 Hz, 1H), 6.54 (d, J = 1.7 Hz, 1H), 2.88 (s, 6H); ^{13}C NMR (126 MHz, pyridine) δ 180.9, 154.3, 147.6, 144.4, 133.2, 133.0, 132.5, 132.2, 130.2, 127.2, 110.6, 97.8, 40.4. FT-IR (KBr): 3436, 2913, 2847, 2809, 1616, 1583, 1546, 1454, 1437, 1356, 1276, 1198, 1132, 1081, 1002; HRMS m/z for $C_{14}H_{13}N_2O_3$ [M+H]+ calcd 257.0921, found 257.0920.

5.3. Methyl 7-(dimethylamino)-4-hydroxy-3-oxo-3H-phenoxazine-1-carboxylate, ***4b***

200 mg of methyl gallate (1.09 mmol) and 245 mg of freshly prepared *N,N*-dimethyl-4-nitrosoaniline hydrochloride (1.31 mmol) were added in 10 mL of methanol. The reaction mixture was refluxed for 6 h, while the solution was turning into purple color. Then, the reaction mixture was cooled, the crystals were collected by suction filtration on a filter paper and were washed with chilled MeOH. The solid was dried under reduced pressure to give 192 mg of **4b** as a dark purple solid in 56% yield. **4b**: mp > 300 °C, ^{1}H NMR (500 MHz, DMSO-*d6*/pyridine-*d5*) δ 7.52 (d, J = 9.1 Hz, 1H), 7.01 (s, 1H), 6.81 (dd, J = 9.1, 2.5 Hz, 1H), 6.62 (d, J = 2.5 Hz, 1H), 3.86 (s, 3H), 3.09 (s, 6H); ^{13}C NMR (126 MHz, DMSO-*d6*/pyridine-*d5*) δ 176.9, 165.3, 154.2, 146.3, 137.9, 135.1, 133.6, 131.7, 131.74, 127.3, 125.9, 111.1, 96.3, 52.5 (1 carbon missing due to overlapping with DMSO-d6); FT-IR (KBr): 3435, 3046, 1707, 1599, 1547, 1433, 1413, 1383, 1315, 1247, 1190, 1140, 985, 850; HRMS m/z for $C_{16}H_{15}N_2O_5^{+}$ [M+H]$^{+}$ calcd 315.0975, found 315.0975.

5.4. Ethyl 7-(dimethylamino)-4-hydroxy-3-oxo-3H-phenoxazine-1-carboxylate, ***4c***

200 mg of ethyl gallate (1.01 mmol) and 225 mg of freshly prepared *N,N*-dimethyl-4-nitrosoaniline hydrochloride (1.21 mmol) were added in 3.5 mL of ethanol. The reaction mixture was refluxed for 1 h, while the solution was turning into purple color. Then, the reaction mixture was cooled, the crystals were collected by suction filtration on a filter paper and were washed with chilled EtOH. The solid was recrystallized with EtOH and was dried under reduced pressure to give 106 mg of **4c** as dark purple solid (32% yield). **4c:** mp > 300 °C, ^{1}H NMR (500 MHz, pyridine-*d5*) δ 7.68 (d, J = 9.1 Hz, 1H), 7.44 (s, 1H), 6.61 (dd, J = 9.1, 2.5 Hz, 1H), 6.50 (d, J = 2.5 Hz, 1H), 4.45 (q, J = 7.1 Hz, 2H), 2.84 (s, 6H), 1.30 (t, J = 7.1 Hz, 3H); ^{13}C NMR (126 MHz, pyridine-*d5*) δ 179.2, 166.2, 154.8, 147.6, 140.6, 137.5, 135.5, 133.1, 132.7, 129.3, 127.3, 111.3, 97.4, 62.3, 40.4, 14.8; FT-IR (KBr): 3437, 3071, 2994, 2928, 1699, 1601, 1547, 1491, 1463, 1420, 1383, 1315, 1266, 1241, 1196; HRMS m/z for $C_{17}H_{17}N_2O_5$ [M+H]+ calcd 329.1132, found 329.1131.

5.5. N-(9-(Ethoxycarbonyl)-6,7-dihydroxy-3H-phenoxazin-3-ylidene)-N-methylmethanaminium chloride, ***5c***

30 μL of HCl in *i*PrOH (5N) solution were added dropwise in a suspension of ethyl 7-(dimethylamino)-4-hydroxy-3-oxo-3H-phenoxazine-1-carboxylate, **4c** (10 mg, 0.03 mmol) in 0.6 mL of ethanol. The mixture was stirred at room temperature for 30 min. Then, the mixture was concentrated to furnish **5c** (quantitative yield) as a dark blue-green solid. **5c:** mp > 300 °C; ^{1}H NMR (500 MHz, DMSO-*d6*) δ 7.52 (d, J = 9.6 Hz, 1H), 6.98 (s, 2H), 6.72 (s,

1H), 4.33 (q, J = 7.1 Hz, 2H), 3.20 (s, 6H), 1.31 (t, J = 7.1 Hz, 3H); HRMS m/z for $C_{17}H_{17}N_2O_5$ [M]+ calcd 329.1132, found 329.1132.

5.6. Isopropyl 7-(dimethylamino)-4-hydroxy-3-oxo-3H-phenoxazine-1-carboxylate, **4d**

100 mg of isopropyl gallate (0.475 mmol) and 106 mg of freshly prepared *N,N*-dimethyl-4-nitrosoaniline hydrochloride (0.569 mmol) were added in 4.3 mL of ethanol. The reaction mixture was refluxed for 4 h, while the solution was turning into purple color. The crude product was crystallized with the slow addition of the reaction mixture into 120 mL of water. The crystals were collected by suction filtration on a filter paper and were further purified by flash column chromatography (eluent; ethyl acetate/MeOH = 100/3) to afford 41 mg of **4d** (25% yield) as dark purple solid. **4d:** mp = 232–235 °C; ^{1}H NMR (500 MHz, DMSO-*d6*, 49 °C) δ 7.46 (d, J = 9.1 Hz, 1H), 7.07–6.75 (m, 2H), 6.64 (d, J = 2.0 Hz, 1H), 5.19 (dt, J = 12.5, 6.3 Hz, 1H), 3.15 (s, 6H), 1.34 (d, J = 6.2 Hz, 6H); ^{13}C NMR (126 MHz, DMSO-*d6*) δ 176.8, 164.1, 154.1, 146.1, 137.9, 134.6, 133.9, 131.5, 131.3, 126.6, 125.6, 110.9, 96.2, 68.9, (1 carbon missing due to overlapping with DMSO-d6), 21.3; FT-IR (KBr): 3434, 3232, 2980, 2926, 1703, 1618, 1587, 1533, 1455, 1373, 1332, 1265, 1188, 1123, 1099; HRMS m/z for $C_{18}H_{19}N_2O_5$ [M+H]+ calcd 343.1288, found 343.1288.

5.7. Butyl 7-(dimethylamino)-4-hydroxy-3-oxo-3H-phenoxazine-1-carboxylate, **4e**

200 mg of butyl gallate (0.884 mmol) and 165 mg of freshly prepared *N,N*-dimethyl-4-nitrosoaniline hydrochloride (0.884 mmol) were dissolved in 8 mL of methanol. The reaction mixture was refluxed for 12 h, while the solution was turning into purple-red color. The crystals were collected by suction filtration on a filter paper and were dried under reduced pressure to give 79 mg of **4e**. The filtrate was concentrated and the product was purified by dry silica chromatography (eluent; ethyl acetate/methanol = 100/3) to afford 91 mg of **4e** (total yield 54%). **4e:** mp = 285–287 °C; ^{1}H NMR (500 MHz, DMSO-*d6*) δ 9.46 (s, 1H), 7.45 (d, J = 8.4 Hz, 1H), 6.91 (s, 1H), 6.89 (m, 1H), 6.65 (s, 1H), 4.29 (t, J = 6.3 Hz, 2H), 3.15 (s, 6H), 1.83–1.54 (m, 2H), 1.46 (m, 2H), 0.94 (t, J = 7.4 Hz, 3H); ^{13}C NMR (126 MHz, DMSO-*d6*) δ 177.0, 165.0, 154.3, 146.3, 137.9, 133.8, 131.7, 131.5, 127.0, 125.9, 111.3, 108.5, 96.3, 65.0, 40.2, 30.1, 18.6, 13.6; FT-IR (KBr): 3247, 2957, 2924, 2860, 1716, 1614, 1586, 1536, 1489, 1455, 1375, 1330, 1260, 1186, 1117; HRMS m/z for $C_{19}H_{21}N_2O_5$ [M+H]+ calcd 357.1445, found 357.1444.

5.8. N-(9-(Butoxycarbonyl)-6,7-dihydroxy-3H-phenoxazin-3-ylidene)-N-methylmethanaminium chloride, **5e**

28 μL of HCl in iPrOH (5N) solution were added dropwise in a suspension of butyl 7-(dimethylamino)-4-hydroxy-3-oxo-3*H*-phenoxazine-1-carboxylate **4e** (10 mg, 0.028 mmol) in 0.6 mL of ethanol. The mixture was stirred at room temperature for 30 min. Then, the mixture was concentrated to furnish **5e** (quantitative yield) as a dark blue-green solid. **5e:** mp = 163–166 °C; ^{1}H NMR (500 MHz, DMSO-*d6*, 49 °C) δ 7.55 (d, J = 9.3 Hz, 1H), 7.16 (d, J = 7.8 Hz, 1H), 7.10 (s, 1H), 6.83 (s, 1H), 4.32 (t, J = 6.3 Hz, 2H), 3.29 (s, 6H), 1.70 (m, 2H), 1.48 (m, 2H), 0.96 (t, J = 7.4 Hz, 3H); HRMS m/z for $C_{19}H_{21}N_2O_5$ [M]+ calcd 357.1445, found 357.1442.

5.9. Benzyl 7-(dimethylamino)-4-hydroxy-3-oxo-3H-phenoxazine-1-carboxylate, **4f**

50 mg of benzyl gallate (0.192 mmol) and 42 mg of freshly prepared *N,N*-dimethyl-4-nitrosoaniline hydrochloride (0.223 mmol) were dissolved in 1.7 mL of ethanol. The reaction mixture was refluxed for 3 h, while the solution was turning into purple color. The crude product was crystallized with the slow addition of the reaction mixture into 48 mL of water. The crystals were collected by suction filtration on a filter paper and were further purified by flash column chromatography (eluent; ethyl acetate/MeOH = 100/5) to afford 26 mg of **4f** (35% yield) as a dark purple solid. **4f**: mp = 221–224 °C; ^{1}H NMR (500 MHz, DMSO-*d6*) δ 9.49 (s, 1H), 7.53 (d, J = 7.3 Hz, 2H), 7.47 (d, J = 9.1 Hz, 1H), 7.42 (t, J = 7.4 Hz, 2H), 7.36 (t, J = 7.4 Hz, 1H), 6.97 (s, 1H), 6.89 (d, J = 8.4 Hz, 1H), 6.66 (s, 1H), 5.38 (s, 2H), 3.16 (s, 6H); ^{13}C NMR (126 MHz, pyridine-*d5*, 40 °C) δ 179.0, 166.2, 154.9, 147.6, 140.6, 137.5, 137.1, 135.1, 133.1, 132.6, 129.6, 129.3, 129.0, 127.3, 111.4, 97.4, 67.9, 40.4 (one carbon missing due to overlapping); FT-IR (KBr): 3205, 2923, 2847, 1728, 1618, 1577, 1521, 1493, 1456, 1387, 1362, 1232, 1209, 1178, 1137, 1115, 1020; HRMS m/z for $C_{22}H_{19}N_2O_5$ [M+H]+ calcd 391.1288, found 391.1294.

5.10. 2-Methoxyethyl 7-(dimethylamino)-4-hydroxy-3-oxo-3H-phenoxazine-1-carboxylate, **4g**

50 mg of 2-methoxyethyl gallate (0.219 mmol) and 47 mg of freshly prepared *N,N*-dimethyl-4-nitrosoaniline hydrochloride (0.254 mmol) were dissolved in 2 mL of ethanol. The reaction mixture was refluxed for 3.30 h, while the solution was turning into purple color. Then, the reaction mixture was cooled, the crystals were collected by suction filtration on a filter paper and dried under reduced pressure to give 25 mg of **4g** as a dark purple solid in 32% yield. **4g**: mp > 300 °C, ^{1}H NMR (500 MHz, DMSO-*d6*) δ 7.66 (d, J = 9.5 Hz, 1H), 7.33 (m, 1H), 7.25 (s, 1H), 6.95 (d, J = 1.8 Hz, 1H), 4.50–4.39 (m, 2H), 3.72–3.62 (m, 2H), 3.37 (s, 6H), 3.31 (s, 3H); ^{13}C NMR (126 MHz, DMSO-*d6*/pyridine-*d5*, 49 °C) δ 176.8, 164.5, 154.1, 146.1, 137.9, 133.4, 133.1, 131.5, 127.3, 125.8, 114.1, 110.9, 96.1, 69.5, 64.2, 57.9 (one carbon missing due to overlapping); FT-IR (KBr): 3433, 2923,1719, 1599, 1548, 1485, 1425, 1382, 1316, 1279, 1247, 1212, 1191, 1122, 1094; HRMS m/z for $C_{18}H_{19}N_2O_6$ $[M+H]^+$ calcd 359.1238, found 359.1237.

5.11. N-(6,7-Dihydroxy-9-((2-methoxyethoxy)carbonyl)-3H-phenoxazin-3-ylidene)-N-methylmethanaminium chloride, **5g**

28 μL of HCl in iPrOH (5N) solution were added dropwise in a suspension of 2-methoxyethyl 7-(dimethylamino)-4-hydroxy-3-oxo-3H-phenoxazine-1-carboxylate **4g** (10 mg, 0.028 mmol) in 0.6 mL of ethanol. The mixture was stirred at room temperature for 30 min. Then, the mixture was concentrated to furnish **5g** (quantitative yield) as a dark blue-green solid. **5g**: mp = 188–191 °C ^{1}H NMR (500 MHz, DMSO-*d6*, 49 °C) δ 7.54 (d, J = 9.2 Hz, 1H), 7.09–6.91 (m, 2H), 6.74 (d, J = 2.5 Hz, 1H), 4.61–4.25 (t, J = 5.0 Hz, 2H), 3.88–3.58 (t, J = 5.0 Hz, 2H), 3.32 (s, 3H), 3.22 (s, 6H); HRMS m/z for $C_{18}H_{19}N_2O_6$ $[M]^+$ calcd 359.1238, found 359.1238.

5.12. Hexyl 7-(dimethylamino)-4-hydroxy-3-oxo-3H-phenoxazine-1-carboxylate, **4h**

59 mg of hexyl gallate (0.233 mmol) and 52 mg of freshly prepared *N,N*-dimethyl-4-nitrosoaniline hydrochloride (0.28 mmol) were dissolved in 0.8 mL of ethanol. The reaction mixture was refluxed for 1 h, while the solution was turning into purple color. The crude product was crystallized with the slow addition of the reaction mixture into 100 mL of water. The crystals were collected by suction filtration on a filter paper and were further purified by flash column chromatography (eluent; ethyl acetate/MeOH = 100/3) to afford 30 mg of **4h** (33% yield) as a dark purple solid. **4h:** mp = 186–189 °C,^{1}H NMR (500 MHz, DMSO-*d6*/pyridine-*d5*) δ 7.47

(d, J = 9.1 Hz, 1H), 6.98 (s, 1H), 6.83 (d, J = 8.6 Hz, 1H), 6.63 (s, 1H), 4.29 (t, J = 6.4 Hz, 2H), 3.10 (s, 6H), 1.81–1.59 (m, 2H), 1.38 (m, 2H), 1.24 (m, 4H), 0.81 (s, 3H); ^{13}C NMR (126 MHz, DMSO-*d6*/pyridine-*d5*) δ 177.0, 165.0, 154.2, 146.3, 138.0, 133.8, 131.6, 127.1, 125.9, 111.1, 96.3, 65.3, 45.7, 30.8, 28.0, 25.0, 22.0, 13.8 (two carbons are missing due to overlapping with pyridine-*d5*); FT-IR (KBr): 3454, 2955, 2844, 1726, 1582, 1457, 1428, 1336, 1242, 1188, 1111; HRMS *m/z* for $C_{21}H_{25}N_2O_5$ [M+H]+ calcd 385.1758, found 385.1762.

5.13. N-(9-((Hexyloxy)carbonyl)-6,7-dihydroxy-3H-phenoxazin-3-ylidene)-N-methylmethan-aminium chloride, **5h**

26 μL of HCl in *i*PrOH (5N) solution were added dropwise in a suspension of hexyl 7-(dimethylamino)-4-hydroxy-3-oxo-3H-phenoxazine-1-carboxylate **4h** (10 mg, 0.026 mmol) in 0.6 mL of ethanol. The mixture was stirred at room temperature for 30 min. Then, the mixture was concentrated to furnish **5h** (quantitative yield) as a dark blue-green solid. **5h:** mp = 175–178 °C, ^{1}H NMR (500 MHz, DMSO-*d6*, 49 °C) δ 7.50 (d, J = 9.3 Hz, 1H), 7.00 (dd, J = 9.4, 2.2 Hz, 1H), 6.97 (s, 1H), 6.73 (d, J = 2.7 Hz, 1H), 4.30 (t, J = 6.4 Hz, 2H), 3.22 (s, 6H), 1.78–1.68 (m, 2H), 1.55–1.37 (m, 2H), 1.33 (s, 4H), 0.89 (d, J = 6.9 Hz, 3H); HRMS *m/z* for $C_{21}H_{25}N_2O_5$ [M]+ calcd 385.1758, found 385.1760.

5.14. 7-(Dimethylamino)-1-methyl-3H-phenoxazine-3-one, **4i**

100 mg of monohydrate orcinol (0.704 mmol) and 160 mg of freshly prepared *N,N*-dimethyl-4-nitrosoaniline hydrochloride (0.844 mmol) were dissolved in 7 mL of methanol. The reaction mixture was refluxed for 12 h, while the solution was turning into purple-red color. The reaction mixture was concentrated under the reduced pressure and was purified by flash column chromatography (eluent; ethyl acetate/MeOH = 100/3) to obtain 82 mg of **4i** as a dark red solid (46% yield). **4i:** mp = 229–232 °C; ^{1}H NMR (500 MHz, $CDCl_3$) δ 7.59 (d, J = 9.1 Hz, 1H), 6.69 (d, J = 8.9 Hz, 1H), 6.61 (s, 1H), 6.43 (s, 1H), 6.18 (s, 1H), 3.14 (s, 6H), 2.40 (s, 3H); ^{13}C NMR (126 MHz, $CDCl_3$) δ 185.9, 153.5, 150.8, 146.6, 142.9, 142.0, 131.6, 130.7, 125.8, 110.3, 105.2, 96.4, 40.4, 16.8; FT-IR (KBr): 2880, 1614, 1547, 1483, 1459, 1413, 1378, 1335, 1287, 1198, 1175, 1135, 900; HRMS *m/z* for $C_{15}H_{15}N_2O_2$ $[M+H]^+$ calcd 255.1128, found 255.1127.

5.15. 7-(Dimethylamino)-1-hydroxy-3H-phenoxazin-3-one, **4j**

N,N-dimethyl-4-nitroso aniline (345 mg, 1.85 mmol) and phloroglucinol (200 mg, 1.23 mmol) were heated under reflux in ethanol (15.5 mL) for 2.5 h. The mixture was allowed to cool at 0 °C. The precipitate was collected by filtration and washed with ethanol (3 × 1 ml), to obtain 128 mg of **4j** as a dark blue-purple product (40% yield) [37]. **4j:** mp > 300 °C, ^{1}H NMR (500 MHz, pyridine-d5) δ 7.56 (d, J = 9.0 Hz, 1H), 6.63 (d, J = 2.0 Hz, 1H), 6.61 (dd, J = 9.1, 2.6 Hz, 1H), 6.46 (d, J = 2.6 Hz, 1H), 2.91 (s, 6H); ^{13}C NMR (126 MHz, pyridine-d5) δ 186.4, 159.3, 154.2, 147.6, 138.7, 131.5, 125.3, 110.7, 109.5, 104.2, 97.4, 40.2 (one carbon is missing due to overlapping); FT-IR (KBr): 3389, 2879, 1649, 1612, 1576, 1536, 1480, 1390, 1327, 1279, 1213, 1157, 1083, 900, 846; HRMS *m/z* for $C_{15}H_{13}N_2O_3$ $[M+H]^+$ calcd 257.0921, found 257.0920.

5.16. Methyl 7-(dipropylamino)-4-hydroxy-3-oxo-3H-phenoxazine-1-carboxylate, **7b**

63 mg of methyl gallate (0.343 mmol) and 100 mg of freshly prepared *N,N*-dipropyl-4-nitrosoaniline hydrochloride (0.412 mmol) were dissolved in 1.2 mL of ethanol. The reaction mixture was refluxed for 1.5 h, while the solution was turning into purple color. The crude product was crystallized with the slow addition of the reaction mixture into 84 mL of water. The crystals were collected by suction filtration on a filter paper and were further purified by flash column chromatography (eluent; ethyl acetate/MeOH = 100/3) to afford 32 mg of **7b** (33% yield) as a dark purple solid. **7b:** mp = 223–225 °C; ^{1}H NMR (500 MHz, $CDCl_3$) δ 7.62 (d, J = 9.3 Hz, 1H), 7.21 (s, 1H), 6.73 (dd, J = 9.3, 2.5 Hz, 1H), 6.58 (d, J = 2.5 Hz, 1H), 3.98 (s, 3H), 3.77–3.03 (m, 4H), 1.72 (m, 4H), 1.00 (t, J = 7.4 Hz, 6H); ^{13}C NMR (126 MHz, $CDCl_3$) δ 176.5, 165.5, 153.4, 146.9, 137.5, 134.0, 133.4, 133.3, 130.9, 127.4, 127.3, 111.3, 96.3, 53.4, 52.8, 20.6, 11.3; FT-IR (KBr): 3451, 3224, 2970, 2872, 1728, 1612, 1585,1534, 1457, 1401, 1364,1335, 1305, 1232, 1203, 1172, 1114; HRMS *m/z* for $C_{20}H_{23}N_2O_5$ $[M+H]^+$ calcd 371.1601, found 371.1601.

5.17. Butyl 7-(dipropylamino)-4-hydroxy-3-oxo-3H-phenoxazine-1-carboxylate **7e**

117 mg of butyl gallate (0.515 mmol) and 150 mg of freshly prepared *N,N*-dipropyl-4-nitrosoaniline hydrochloride (0.628 mmol) were dissolved in 1.8 mL of ethanol. The reaction mixture was refluxed for 1.5 h, while the solution was turning into purple color. The crude product was crystallized with the slow addition of the reaction mixture into 126 mL of water. The crystals were collected by suction filtration on a filter paper and were further purified by flash column chromatography (eluent; ethyl acetate/MeOH = 100/3) to afford 63 mg of **7e** (30% yield) as a dark purple solid. **7e:** mp = 102–105 °C; ^{1}H NMR (500 MHz, $CDCl_3$) δ 7.58 (d, J = 9.2 Hz, 1H), 7.17 (s, 1H), 6.69 (d, J = 9.2 Hz, 1H), 6.56 (s, 1H), 4.39 (t, J = 8.0 Hz, 2H), 3.46–3.29 (t, J = 10.0 Hz 4H), 1.74 (m, 6H), 1.52 (m, 2H), 0.99 (m, 9H); ^{13}C NMR (126 MHz, $CDCl_3$) δ 176.7, 165.2, 153.3, 146.9, 137.7, 133.7, 133.2, 130.9, 127.3, 127.2, 111.2, 96.3, 65.6, 53.4, 30.6, 20.6, 19.2, 13.7, 11.3 (one carbon is missing due to overlapping); FT-IR (KBr): 3442, 2961, 2927, 2850, 1628, 1587, 1520, 1451, 1396, 1356, 1232, 1115; HRMS *m/z* for $C_{23}H_{29}N_2O_5$ $[M+H]^+$ calcd 413.2071, found 413.2070.

5.18. Cell culture and preparation of mouse primary cortical neurons

HEK-293 human embryonic kidney cells overexpressing LRP6 (HEK-293LRP6) or DKK1 (HEK-293DKK1) were cultured in a 5% CO_2 atmosphere at 37 °C in Dulbecco's Modified Eagle's Medium (DMEM) (Sigma Aldrich, Athens, Greece) supplemented with 10% heat inactivated fetal bovine serum (FBS) (PAA Laboratories GmbH, Linz, Austria), 1% penicillin/streptomycin (Sigma Aldrich, Athens, Greece) and 10 μg/ml Blasticidine for HEK-293DKK1 and 100 μg/ml Zeocine for HEK-293LRP6. Confluent HEK-293DKK1 cells were cultured for 72 h and the conditioned medium was collected, cleared from cell debris and floating cells by centrifugation and stored at −80 °C until use. Primary mouse cortex neuronal culture were prepared from 16 days embryos as described and were treated with PG J2 after 6 days in vitro [38].

5.19. DKK1 binding assay

Binding of DKK1 was performed as previously described by Iozzi and coworkers [15]. Briefly, HEK-293-LRP6 cells were seeded onto poly-D-lysine-coated coverslips 24 h before the experiment and were incubated with DKK1 conditioned media (DKK1-CM) plus DMSO, DKK1-CM plus NCI8642 (100 μM) or DKK1-CM plus NCI8642 derivatives (100 μM) for 2 h at 4 °C. After washing, the cells was fixed in 3% paraformaldehyde (15 min, room temperature), blocked with PBS/0.1% BSA, and incubated with the primary rabbit-anti-DKK1 antibody, and fluorescent secondary antibody Alexa488 diluted into blocking solution. This antibody which emits fluorescence at 519 nM was very carefully chosen following the

observation that some of the NCI8642 derivatives emit fluorescence at 570 nM. Cell nuclei were counterstained with DAPI. Images were collected using a fluorescence microscope and 750 cells were analyzed each time using ZEN software.

5.20. Cell treatments and cell lysis

Mouse cortex primary neurons were treated with 20 μM prostaglandin J2 and DMSO, 10 μM NCI8642 or 10 μM NCI8642 derivatives for 1 h at 37 °C.

Following treatment, cells were lysed at 4 °C in lysis buffer [50 mM Tris–HCl, 150 mM NaCl, 2 mM EDTA, pH 7.6, 1% Triton X-100 (v/v)] supplemented with complete protease inhibitor cocktail and phosphatase inhibitor cocktail (Roche Applied Science, Manheim, Germany). Cell lysates were left on ice for 30 min and then centrifuged at 14,000 g for 12 min at 4 °C. Protein concentrations in supernatants were determined by using the Bradford protein assay.

5.21. Western blot and densitometry

Appropriate protein concentrations of cell lysates were prepared in Laemmli solubilisation buffer containing β-mercaptoethanol and analyzed by sodium dodecyl sulfate polyacrylamide (SDS-PAGE) gel electrophoresis. Separated proteins were transferred to polyvinyldiene difluoride membranes (Roth GmbH, Karlsruhe, Germany) and immunoblotted with the appropriate dilutions of the primary antibody overnight at 4 °C. Primary antibodies were: Polyclonal rabbit antibody detecting mouse tau phosphorylated at serine396 (1:1000) and a polyclonal antibody directed against the N-terminus of tau (1:1000) that was a kind gift of Dr. Luc Buee (Inserm, Lille, France). The membranes were washed with Tris-buffered Saline-Tween 20 (TBS-T) three times for 5 min and incubated with a 1:5000 dilution of goat anti-rabbit or anti-mouse horseradish peroxidise-conjugated secondary antibodies for 1 h at room temperature. Following washing with TBS-T, proteins were detected by chemiluminescence using the enhanced chemiluminescence system (GenScript Piscataway, NJ, USA) on a Fluorochem 8800 imaging station (AlphaInnotech, CA, USA). TIFF files of the images were viewed in ImageJ and band intensity was quantified with ImageJ software. The intensity measurements of the bands were normalized to the levels of actin. The results from three independent experiments were presented in graphs as mean ± SD.

5.22. MTT assay

Primary neuronal cultures were seeded in 96-well plates at a density of 25,000 cells/well and 15,000 cells/well. The cultures were grown for 6 days at 37 °C with 5% CO_2. Then medium was changed to that containing various concentrations (10 μM or 100 μM) of NCI8642 and NCI8642 derivatives and incubated for 24 h at 37 °C with 5% CO_2. In all cases the final concentration of DMSO was 0.1%. 20 μl of MTT reagent (2.5 mg/ml MTT in PBS) was added to each well and incubated for 4 h. The resulting formazan dye was extracted with 100 μl isopropanol/HCl (100 ml isopropanol + 833 μl HCl) and the absorbance was measured spectrophotometrically at a wavelength of 545 nm.

5.23. Statistical analysis

All experiments were repeated three times. One-way ANOVA with Bonferroni's Multiple Comparison Test was used to evaluate the statistical significance of the differences. Statistical significance was defined as $p < 0.05$.

5.24. Molecular docking analysis

Novel leads based on the hit compound NCI8642were designed and rationalized *in silico* prior to synthesis [39]. These compounds form a library of a smile formatted file (*.smi) with the use of the program Open Babel [40], generating their conformers with the Omega v.2.5.1.4 software (OpenEye Scientific Software, Inc., Santa Fe, NM, USA; www.eyesopen.com) [41]. All the docking experiments were performed on a typical desktop pc running Windows 7 64-bit operating system (Dual Core Intel Pentium 3.2 GHz CPU processors, RAM 8 GB), using the OEDocking suite v. 3.0.1 programs (OpenEye Scientific Software, Inc., Santa Fe, NM, USA; www.eyesopen.com) [42–44] and the PyRx v. 0.8 program (The Scripps Research Institute) [45]. Based on the fact that the programs run with different algorithms, a greater probability of the predict model is offered. The visualization of the docking solutions is given by the software PyMol v. 1.4.1 [29].

Molecular descriptor values for the synthesized compounds were also calculated in an effort to export the drug-like profile for them. Those include the factor of sp^3 molecular orbitals (Fsp^3), resembling the compound saturation levels (flatness) [46], Lipinski's rule of five [47,48] descriptors (where calculated logarithmic lipophilicity "clogPMB" was achieved with the use of program Marvin Beans v. 14.9.29) [49,50] and spatial characteristics (volume and polar surface area, see Table 1 in supporting information) were calculated online with the freely available Molinspiration property calculation service (www.molinspiration.com).

5.25. Ligand and protein preparation

The crystal structure of LRP6-E3E4/DKK1 complex (PDB code: 3S8V) was obtained from the protein databank [28]. DKK1 peptide was removed with the use of OEDocking suite program MAKE RECEPTOR v. 3.0.1 (OpenEye Scientific Software, Inc., Santa Fe, NM, USA; www.eyesopen.com) [42–44] and the prepared structure was eventually used as input file for the docking. The search space was centered on the LRP6-E3E4/DKK1 interfaces between subunits A and B. This process generated an initial 40,025 $Å^3$ box, which resulted after a balanced site-shape potential implementation to an outer contour docking space of 13,515 $Å^3$, narrowed by an inner contour docking space of 10,559 $Å^3$. No further residue modifications were made and the docking was performed without any present constraints. The in-house formed library of NCI8642 analogues was collected and the structures were transformed to their smile formatted file (*.smi) with the use of the program Open Babel [40]. Optimal parameters for conformer generation were determined using the Omega v.2.5.1.4 software (OpenEye Scientific Software, Inc., Santa Fe, NM, USA; www.eyesopen.com) [41,42] and the docking experiments were accomplished using of OEDocking suite program FRED v. 3.0.1 (OpenEye Scientific Software, Inc., Santa Fe, NM, USA; www.eyesopen.com) [43–45], utilizing an Exhaustive Search Algorithm. All the results were additionally refined by the use of OEDocking suite program FRED rescore v. 3.0.1 (OpenEye Scientific Software, Inc., Santa Fe, NM, USA; www.eyesopen.com) [43–45] giving the sorting of poses based on its standard options.

5.26. Validation of the docking protocol and ligand docking

The docking was reproduced for the compiled library also with the use of the program AutoDock Vina (The Scripps Research Institute) [51], utilizing this program's Genetic Algorithm. Whilst the protein is treated as rigid and the solely parameter adjustment was observed on the "exhaustiveness", which value was set to 100 instead of the default 8.

Acknowledgment

This programme was implemented within the framework of the Operational Programme «Education and Lifelong Learning» of NSRF: ARISTEIA II. It was co-funded by the European Union and national resources. Furthermore the authors would like to thank Openeye Scientific Software, Inc., Santa Fe, NM, USA; www.eyesopen.com, for providing an academic license of their programs.

Appendix A. Supplementary data

Supplementary data related to this article can be found at http://dx.doi.org/10.1016/j.ejmech.2015.11.024.

References

[1] D.J. Selkoe, Alzheimer's disease, Cold Spring Harb. Perspect. Biol. (2011), http://dx.doi.org/10.1101/cshper spect.a004457.
[2] M. Goedert, M.G. Spillantini, R. Jakes, D. Rutherford, R.A. Crowther, Multiple isoforms of human microtubule-associated protein tau: sequences and localization in neurofibrillary tangles of Alzheimer's disease, Neuron 3 (1989) 519–526.
[3] W. Cerpa, J.A. Godoy, I. Alfaro, G.G. Farías, M.J. Metcalfe, R. Fuentealba, C. Bonansco, N.C. Inestrosa, Wnt-7a modulates the synaptic vesicle cycle and synaptic transmission in hippocampal neurons, J. Biol. Chem. 283 (2008) 5918–5927.
[4] D.P. Hanger, W. Noble, Functional implications of glycogen synthase kinase-3-mediated tau phosphorylation, Int. J. Alzheimers Dis. 2011 (2011) 352805.
[5] a) K.M. Cadigan, M.L. Waterman, TCF/LEFs and Wnt signaling in the nucleus, Cold Spring Harb. Perspect. Biol. 4 (2012) 1–23;
b) C. Liu, Y. Kato, Z. Zhang, V.M. Do, B.A. Yankner, X. He, β-Trcp couples β-catenin phosphorylation-degradation and regulates Xenopus axis formation, Proc. Natl. Acad. Sci. U. S. A. 96 (1999) 6273–6278.
[6] A.M. Zorn, Wnt signalling: antagonistic Dickkopfs, Curr. Biol. 11 (2001) R592–R595.
[7] Y. Kawano, R. Kypta, Secreted antagonists of the Wnt signalling pathway, J. Cell Sci. 116 (2003) 2627–2634.
[8] B.K. Brott, S.Y. Sokol, Regulation of Wnt/LRP signaling by distinct domains of Dickkopf proteins, Mol. Cell Biol. 22 (2002) 6100–6110.
[9] M.C. Rosi, I. Luccarini, C. Grossi, A. Fiorentini, M.G. Spillantini, A. Prisco, C. Scali, M. Gianfriddo, A. Caricasole, G.C. Terstappen, F. Casamenti, Increased Dickkopf-1 expression in transgenic mouse models of neurodegenerative disease, J. Neurochem. 112 (2010) 1539–1551.
[10] A. Caricasole, A. Copani, F. Caraci, E. Aronica, A.J. Rozemuller, A. Caruso, M. Storto, G. Gaviraghi, G.C. Terstappen, F. Nicoletti, Induction of Dickkopf-1, a negative modulator of the Wnt pathway, is associated with neuronal degeneration in Alzheimer's brain, J. Neurosci. 24 (2004) 6021–6027.
[11] I. Cappuccio, A. Calderone, C.L. Busceti, F. Biagioni, F. Pontarelli, V. Bruno, M. Storto, G.T. Terstappen, G. Gaviraghi, F. Fornai, G. Battaglia, D. Melchiorri, S. Zukin, F. Nicoletti, A. Caricasole, Induction of Dickkopf-1, a negative modulator of the Wnt pathway, is required for the development of ischemic neuronal death, J. Neurosci. 25 (2005) 2647–2657.
[12] S.A. Purro, E.M. Dickins, P.C. Salinas, The secreted Wnt antagonist Dickkopf-1 is required for amyloid β-mediated synaptic loss, J. Neurosci. 32 (2012) 3492–3498.
[13] H. Glantschnig, R.A. Hampton, P. Lu, J.Z. Zhao, S. Vitelli, L. Huang, P. Haytko, T. Cusick, C. Ireland, S.W. Jarantow, R. Ernst, N. Wei, P. Nantermet, K.R. Scott, J.E. Fisher, F. Talamo, L. Orsatti, A.A. Reszka, P. Sandhu, D. Kimmel, O. Flores, W. Strohl, Z. An, F. Wang, Generation and selection of novel fully human monoclonal antibodies that neutralize Dickkopf-1 (DKK1) inhibitory function in vitro and increase bone mass in vivo, J. Biol. Chem. 285 (2010) 40135–40147.
[14] R. Nietzki, R. Otto, Zur Kenntniss der Indamine und Indophenole, Chem. Berichte 21 (1888) 1736–1745.
[15] S. Iozzi, R. Remelli, B. Lelli, D. Diamanti, S. Pileri, L. Bracci, R. Roncarati, A. Caricasole, S. Bernocco, Functional characterization of a small-molecule inhibitor of the DKK1-LRP6 interaction, ISRN Mol. Biol. 2012 (2012), http://dx.doi.org/10.5402/2012/823875. Article ID 823875.
[16] X. Li, J. Shan, W. Chang, I. Kim, J. Bao, H.J. Lee, X. Zhang, V.T. Samuel, G.I. Shulman, D. Liu, J.J. Zheng, D. Wu, Chemical and genetic evidence for the involvement of Wnt antagonist Dickkopf2 in regulation of glucose metabolism, Proc. Natl. Acad. Sci. U. S. A. 109 (2012) 11402–11407.
[17] U. Hollstein, Actinomycin. Chemistry and mechanism of action, Chem. Rev. 74 (1974) 625–652.
[18] G. Carr, W. Tay, H. Bottriell, S.K. Andersen, A.G. Mauk, R.J. Andersen, Plectosphaeroic acids A, B, and C, indoleamine 2,3-dioxygenase inhibitors produced in culture by a marine isolate of the fungus Plectosphaerella cucumerina, Org. Lett. 11 (2009) 2996–2999.
[19] T. Shimamoto, A. Tomoda, R. Ishida, K. Ohyashiki, Antitumor effects of a novel phenoxazine derivative on human leukemia cell lines in vitro and in vivo, Clin. Cancer Res. 7 (2001) 704–708.
[20] F. Suzuki, K. Hashimoto, M. Ishihara, G. Westman, K. Samuelsson, M. Kawase, N. Motohashi, H. Sakagami, Tumor-specificity and type of cell death induced by phenoxazines, Anticancer Res. 27 (2007) 4233–4238.
[21] H. Prinz, B. Chamasmani, K. Vogel, K.J. Böhm, B. Aicher, M. Gerlach, E.G. Günther, P. Amon, I. Ivanov, K. Müller, N-benzoylated phenoxazines and phenothiazines: synthesis, antiproliferative activity, and inhibition of tubulin polymerization, J. Med. Chem. 54 (2011) 4247–4263.
[22] K. Hayashi, T. Hayashi, A. Tomoda, Phenoxazine derivatives inactivate human cytomegalovirus, herpes simplex virus-1, and herpes simplex virus-2 in vitro, J. Pharmacol. Sci. 106 (2008) 369–375.
[23] V.H. Frade, M.J. Sousa, J.C. Moura, M.S. Gonçalves, Synthesis of naphtho[2,3-a] phenoxazinium chlorides: structure–activity relationships of these heterocycles and benzo[a]phenoxazinium chlorides as new antimicrobial, Bioorg. Med. Chem. 16 (2008) 3274–3282.
[24] K. Takasu, T. Shimogama, C. Satoh, M. Kaiser, R. Brun, M. Ihara, Synthesis and antimalarial property of orally active phenoxazinium salts, J. Med. Chem. 50 (2007) 2281–2284.
[25] J.F. Ge, C. Arai, M. Yang, Md A. Bakar, J. Lu, N.S. Ismail, S. Wittlin, M. Kaiser, R. Brun, S.A. Charman, T. Nguyen, J. Morizzi, I. Itoh, M. Ihara, Discovery of novel benzo[a]phenoxazine SSJ-183 as a drug candidate for malaria, ACS Med. Chem. Lett. 1 (2010) 360–364.
[26] S. Taniguchi, N. Suzuki, M. Masuda, S. Hisanaga, T. Iwatsubo, M. Goedert, M. Hasegawa, Inhibition of heparin-induced tau filament formation by phenothiazines, polyphenols, and porphyrins, J. Biol. Chem. 280 (2005) 7614–7623.
[27] V. Dostál, M. Kotouček, H. Kalašova, V. Bryndová, J. Šimek, Acid-base equilibria of some 7-dimethylamino-3-phenoxazone derivatives, Collect. Czech. Chem. Commun. 47 (1982) 1588–1596.
[28] Z. Cheng, T. Biechele, Z. Wei, S. Morrone, R.T. Moon, L. Wang, W. Xu, Crystal structures of the extracellular domain of LRP6 and its complex with DKK1, Nat. Struct. Mol. Biol. 18 (2011) 1204–1210.
[29] The PyMOL Molecular Graphics System, Version 1.4.1, Schrödinger, LLC.
[30] S. Kumar, R. Nussinov, Close-range electrostatic interactions in proteins, Chembiochem 3 (2002) 604–617.
[31] G.M. Bennett, E.V. Bell, 2.4-Dinitrobenzaldehyde, Org. Synth. 2 (1943) 223.
[32] A. Alama, Y. Takaguchi, H. Ito, T. Yoshida, S. Tsuboi, Multi-functionalization of gallic acid towards improved synthesis of α- and β-DDB, Tetrahedron 61 (2005) 1909–1918.
[33] S. Takaoka, N. Takaoka, Y. Minoshima, J.-M. Huang, M. Kubo, K. Harada, H. Hioki, Y. Fukuyama, Isolation, synthesis, and neurite outgrowth-promoting activity of illicinin A from the flowers of Illicium anisatum, Tetrahedron 65 (2009) 8354–8361.
[34] K. Cheng, X. Wang, S. Zhang, H. Yin, Discovery of small-molecule inhibitors of the TLR1/TLR2 complex, Angew. Chem. 51 (2012) 12246–12249.
[35] P.P. Ambika Singh, S.M.S. Chauhan, Chemoselective esterification of phenolic acids in the presence of sodium bicarbonate in ionic liquids, Synth. Commun. 38 (2008) 928–936.
[36] T. Mosmann, Rapid colorimetric assay for cellular growth and survival: application to proliferation and cytotoxicity assays, J. Immunol. Methods 65 (1983) 55–63.
[37] P. Kele, X. Li, M. Link, K. Na, A. Herner, K. Lrincz, S. Beni, O.S. Wolfbeis, Clickable fluorophores for biological labeling with or without copper, Org. Biomol. Chem. 7 (2009) 3486–3490.
[38] H.J. Rideout, P. Dietrich, Q. Wang, W.T. Dauer, L. Stefanis, alpha-synuclein is required for the fibrillar nature of ubiquitinated inclusions induced by proteasomal inhibition in primary neurons, J. Biol. Chem. 279 (2004) 46915–46920.
[39] D. Wu, Y. Zhang, P. Liu, X. Li, J. Zhang, J. Shan, D. Engelhardt, Compositions and Methods for Bone Formation and Remodeling European Patent, 2012, p. 19 (EP1758562 B1).
[40] N.M. O'Boyle, M. Banck, C.A. James, C. Morley, T. Vandermeersch, G.R. Hutchison, Open babel: an open chemical toolbox, J. Cheminform. 3 (2011) 33.
[41] P.C. Hawkins, A.G. Skillman, G.L. Warren, B.A. Ellingson, M.T. Stahl, Conformer generation with OMEGA: algorithm and validation using high quality structures from the protein databank and Cambridge structural database, J. Chem. Inf. Model 50 (2010) 572–584.
[42] M.R. McGann, H.R. Almond, A. Nicholls, J.A. Grant, F.K. Brown, Gaussian docking functions, Biopolymers 68 (2003) 76–90.
[43] M. McGann, FRED pose prediction and virtual screening accuracy, J. Chem. Inf. Model 51 (2011) 578–596.
[44] G.B. McGaughey, R.P. Sheridan, C.I. Bayly, J.C. Culberson, C. Kreatsoulas, S. Lindsley, V. Maiorov, J.F. Truchon, W.D. Cornell, Comparison of topological, shape, and docking methods in virtual screening, J. Chem. Inf. Model 47 (2007) 1504–1519.
[45] S. Dallakyan, A. Olson, Small-molecule library screening by docking with PyRx, in: J.E. Hempel, C.H. Williams, C.C. Hong (Eds.), Chemical Biology, Springer, New York, 2015, pp. 243–250.
[46] F. Lovering, J. Bikker, C. Humblet, Escape from flatland: increasing saturation as an approach to improving clinical success, J. Med. Chem. 52 (2009) 6752–6756.
[47] C.A. Lipinski, Lead- and drug-like compounds: the rule-of-five revolution, Drug Discov. Today Technol. 1 (2004) 337–341.
[48] C.A. Lipinski, F. Lombardo, B.W. Dominy, P.J. Feeney, Experimental and

computational approaches to estimate solubility and permeability in drug discovery and development settings, Adv. Drug Deliv. Rev. 46 (2001) 3–26.
[49] Marvin, Marvin was used for Drawing, Displaying and Characterizing Chemical Structures, Substructures and Reactions, Marvin 14.9.29, ChemAxon, 2014. http://www.chemaxon.com.
[50] C. Plugins, Calculator Plugins were used for Structure Property Prediction and Calculation, Marvin 14.9.29, ChemAxon, 2014. http://www.chemaxon.com.
[51] O. Trott, A.J. Olson, AutoDock Vina: improving the speed and accuracy of docking with a new scoring function, efficient optimization, and multithreading, J. Comput. Chem. 31 (2010) 455–461.